MOPITT

Measurement of Pollution in the Troposphere

LEVEL 1
ALGORITHM THEORETICAL BASIS DOCUMENT (ATBD)

Conversion of MOPITT Digital Counts into Calibrated Radiances
(Level 0 to Level 1)

University of Toronto and
NCAR (National Center for Atmospheric Research) MOPITT Team

Version 10.0
2025

Table of Contents

1.0 Introduction

This document outlines the theoretical basis of the Measurement of Pollution in the Troposphere (MOPITT) L0 to L1 data processing algorithm . It describes the physics and mathematics of the algorithms that convert the instrument output from raw digital counts (Level 0 data) to calibrated radiances that are geolocated over the globe (Level 1 data). The Level 0 inputs to these algorithms are:

• The telemetered instrument outputs, including those from the detectors, all temperature, pressure, time and angle sensors, and other monitors of instrument state and performance.
• Data on the spacecraft position and attitude as a function of time.

The Level 1 outputs from these algorithms will subsequently be used as inputs to the algorithms that retrieve vertical profiles of carbon monoxide, and total column amounts of carbon monoxide (Level 2 data). The algorithms that create the Level 2 data from the Level 1 data are discussed in a separate ATBD. The algorithms described here apply to the version 10 MOPITT processing. Data processing of L0 to L1 to L2 is performed at the NCAR MOPITT SIPS (Science Investigator-led Processing System).

2.0 Overview and Background

2.1 Experimental Objective

The MOPITT experiment has been described by Drummond (1992), with on-orbit performance illustrated in Drummond et al. (2010) The primary objective of the MOPITT investigation is to enhance our knowledge of the chemistry of the troposphere, and particularly how it interacts with the surface/ocean/biomass systems, atmospheric transport, and the carbon cycle. Before launch, focus was the time evolution of the distribution of carbon monoxide (CO) and methane (CH4) in the troposphere; however, for reasons described in Pfister et al., 2005, the MOPITT methane product is problematic.

For CO, the objective is to obtain profiles with a resolution of 22 km horizontally, 4 km vertically and with an accuracy of 10 % throughout the troposphere. Total column measurements are produced from both thermal infrared profiles and near-infrared observations, as well from combined multispectral profiles. The global distributions of these profiles and column amounts have been used in numerous studies of these gases on a global basis, providing the first detailed information on their horizontal, vertical and temporal variations, and their relationships to other activities such as biomass burning, industrial and transport activity. They are also used in parallel modelling efforts to advance our understanding of global tropospheric chemistry and its relationship to sources, sinks, and atmospheric transport, which can be determined from other data.

2.2 Instrument Characteristics

Drummond (1992) has outlined the MOPITT instrument, and the measurement concept and principles of correlation radiometry are outlined here. The approach and viewing geometry are shown in Figure 2.2.1. MOPITT, on the Terra platform, measures upwelling thermal emission

from the atmosphere and surface and solar radiation that has passed through the atmosphere, been reflected at the surface, and is transmitted back up through the atmosphere.

Measurement of the transmittance of reflected sunlight provides a convenient way to determine the total column amount of a trace gas. In order for this to work, the gas must have a spectral band in a region with large solar radiance, and for which the total optical depth along such a path is not too large. Methane has a set of overtone and combination bands near 2.2 μm which provide a measurable but not overly large total absorption for such a path. For carbon monoxide, the first overtone band, at 2.3 μm, is suitable for a total column measurement.

For vertical profiling, the requirement is that significant and measurable portions of the signal must originate in different atmospheric layers, which means that there must be a few values of different but appreciable opacity in the atmosphere, and that there must also be a source of radiation in the atmosphere. With thermal emission as a radiation source, the CO fundamental band at 4.7 μm experiences enough opacity to determine atmospheric amounts, as demonstrated by Reichle et al. (1986, 1990).

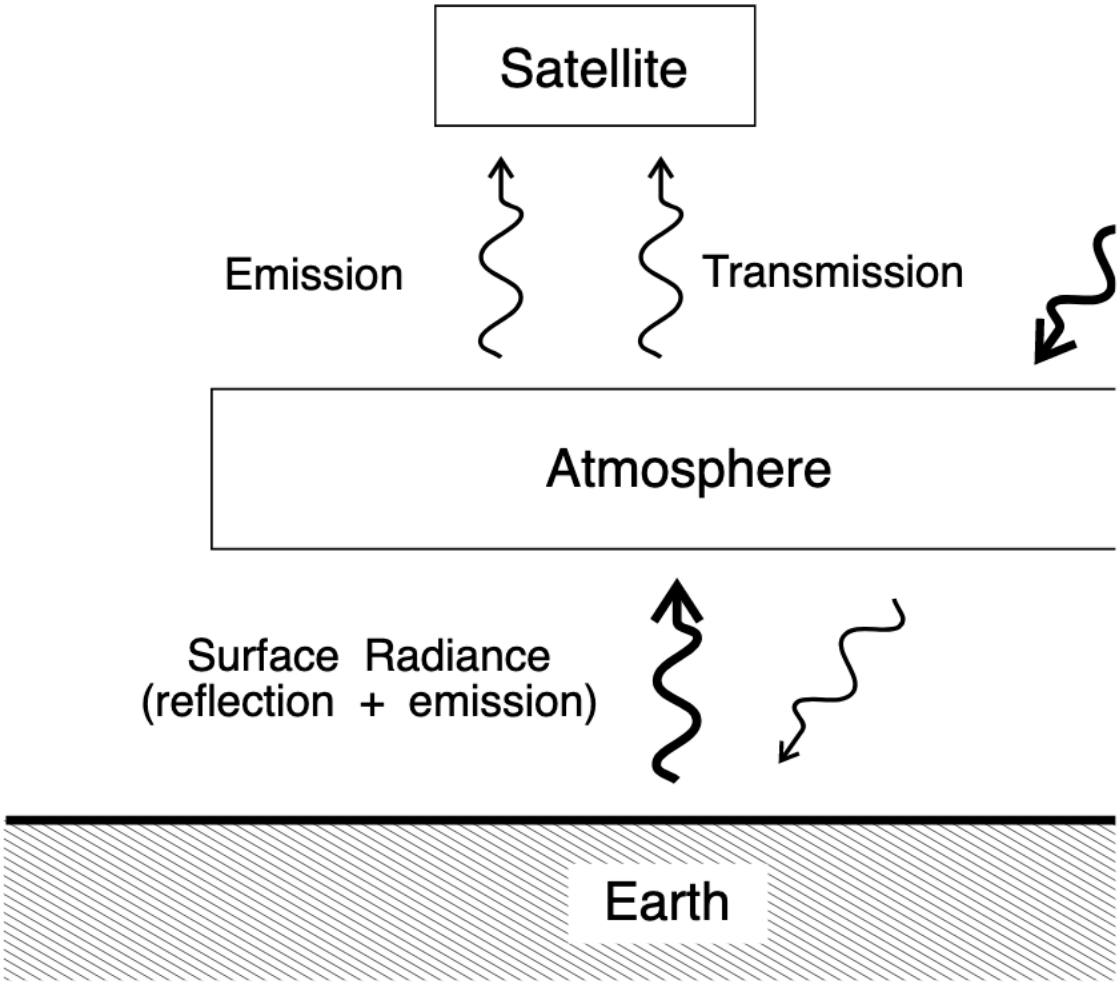

Figure 2.2.1 Schematic of satellite observed radiance from earth emission and solar reflection as transmitted through the atmosphere.

All three of these bands are in regions of the spectrum with other gas bands, and the lines of interest are mixed with those of interfering species. In principle it is possible to measure total emission or transmission in a spectral band, and then correct for the contributions of the interfering species to arrive at a measurement of the species of interest. However, the contributions of the other species are considerably larger than those of the gases of interest, and their amounts are often not known with sufficient accuracy. The uncertainties of the corrections may significantly degrade, or even mask, the detection of changes in the gas of interest.

The MOPITT approach to meeting this challenge is to enhance the sensitivity of the instrument to the gas of interest. Since all gases in the atmosphere are emitting/absorbing simultaneously it is essential that we be able to separate out the effect of the gas of interest from the general radiation field. Further, since we shall see that the information about the height distribution of the gases is contained within the shape of an individual absorption/emission line, it is necessary to be able to resolve the line shape in some manner.

There is, however, a fundamental problem, since the above implies high dispersion to separate the fine details of the spectrum. With high dispersion comes low sensitivity and high precision requirements that are difficult to implement in a space-based instrument. Correlation Radiometry (CR) offers the opportunity for high selectivity without the attendant low sensitivity and high precision requirements.

The fundamental techniques of correlation radiometry are illustrated using the apparatus illustrated in Figure 2.2.2. The cell contains a sample of the gas under consideration. If monochromatic radiation enters from the left and is detected by the system on the right then the output as a function of spectral frequency is shown in Figure 2.2.3(top) for two different amounts of gas in the absorption cell. By cycling the amount of gas in the absorption cell between the two states, the detector will be alternately looking through two different filters. If the difference of the two signals is taken, this signal will be identical to the output of a system in which the gas cell and its modulator are replaced by an optical filter of profile shown by the Effective Difference Transmission (EDT) curve in Figure 2.2.3(middle).

Note that this apparatus has the following properties:

- The "equivalent filter profile" approaches zero between the spectral lines of the gas in the cell, eliminating signals from most of the spectrum.
- The filter profile has a maximum at each spectral line and therefore the energy from each spectral line in a broadband emission is seen simultaneously. The system is therefore very sensitive to radiation with a spectrum identical or similar to that of the gas in the cell. Evidently the spectrum of the gas itself is the best correlated with the filter profile.
- The apparatus contains no high precision optical adjustments. Quantum mechanics keeps the spectra aligned. In fact the only phenomena which affects the alignment is Doppler shifting of the cell and the emission spectrum. The effect of the filter is shown in Figure 2.2.3(bottom) where it can be seen that the spectral emission from lines coincident with

spectral lines of the gas in the cell (even if they originate from another gas) is detected and other emission lines are suppressed.

- Although not shown explicitly here, if small amounts of gas are placed in the cell, the spectral lines will be narrow, with incomplete absorption at the centers of the lines. The EDT will be largest at the line centers, where absorption coefficients are largest. If larger amounts of gas are in the cell, the lines will be broader and completely absorbed in the centers. In this case, the differences will be larger in the line wings, where absorption coefficients are smaller.

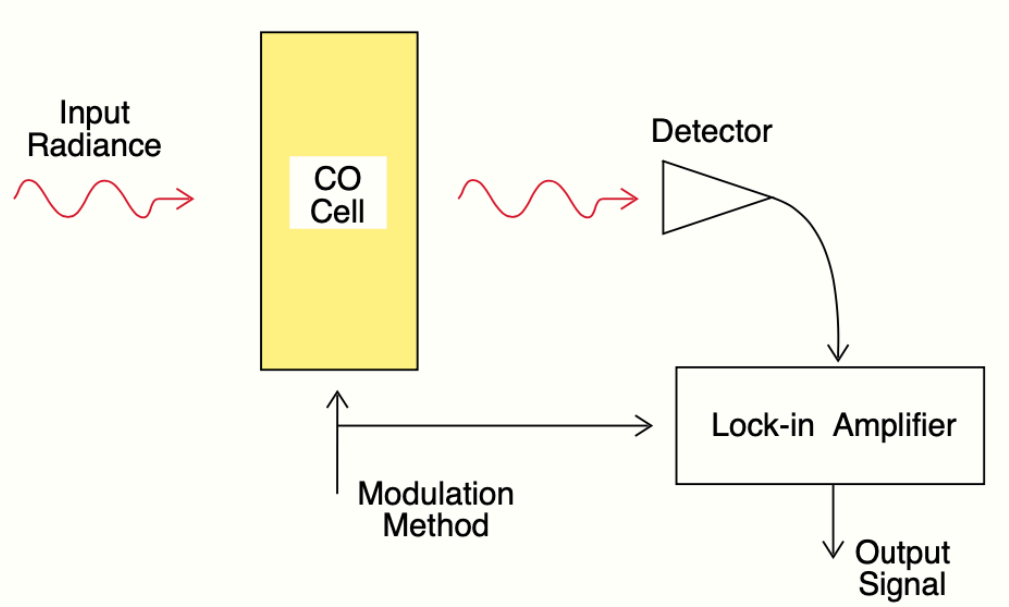

Figure 2.2.2 A basic correlation radiometry system.

The largest part of the upwelling signal emitted by the atmosphere comes from the altitude region in which the optical depth is near unity. Thus, a cell that is sensitive to the line center will respond to signals originating higher in the atmosphere, while a cell with larger amounts of gas will respond to signals originating in the wings of the pressure broadened lines, corresponding to lower altitudes.

The average of the signals obtained at the two states of the CR cell can also be obtained. The resulting Effective Average Transmittance (EAT) is also shown in Figure 2.3.3(middle). It has the property that its transmittance is near unity away from the lines in the cell, but it reduces the signals at the centers of the lines. Thus, it is sensitive to other gases and especially to the surface contribution to the upwelling radiation in the spectral regions considered here.

MOPITT makes use of two methods to modulate the gas transmittance. The first is by pressure modulation, through use of pressure modulated cells (PMC's), which have been described by Taylor (1983). The second is by modulating the length of the gas cell in the optical path, through

length modulated cells (LMC's), which have been described by Drummond (1989). The MOPITT optical arrangement, shown in Figure 2.2.4, employs 2 pressure modulated radiometers (PMR's) with different mean pressures, and 4 length modulated radiometers (LMR's). Dichroic filters are used to separate the 2.2 μm and 2.3 μm channels from the 4.7 μm channels, thus producing a total of 8 separate channels. The characteristics of the channels are given in Table 2.2.1. Each produces an Average (A) and Difference (D) signal. It is the outputs of these radiometers that must be calibrated and geolocated.

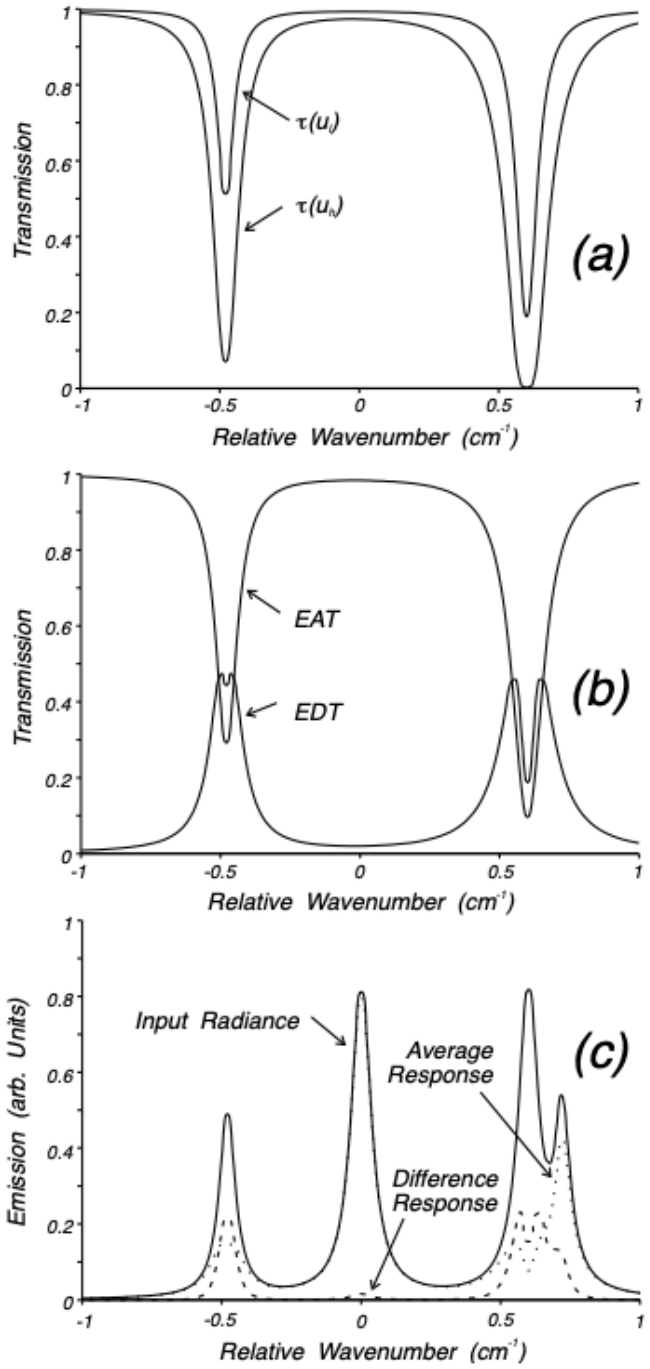

Figure 2.2.3 Operation of a correlation spectrometer in spectral space. EAT is the Equivalent Average Transmission. EDT is the Equivalent Difference Transmission.

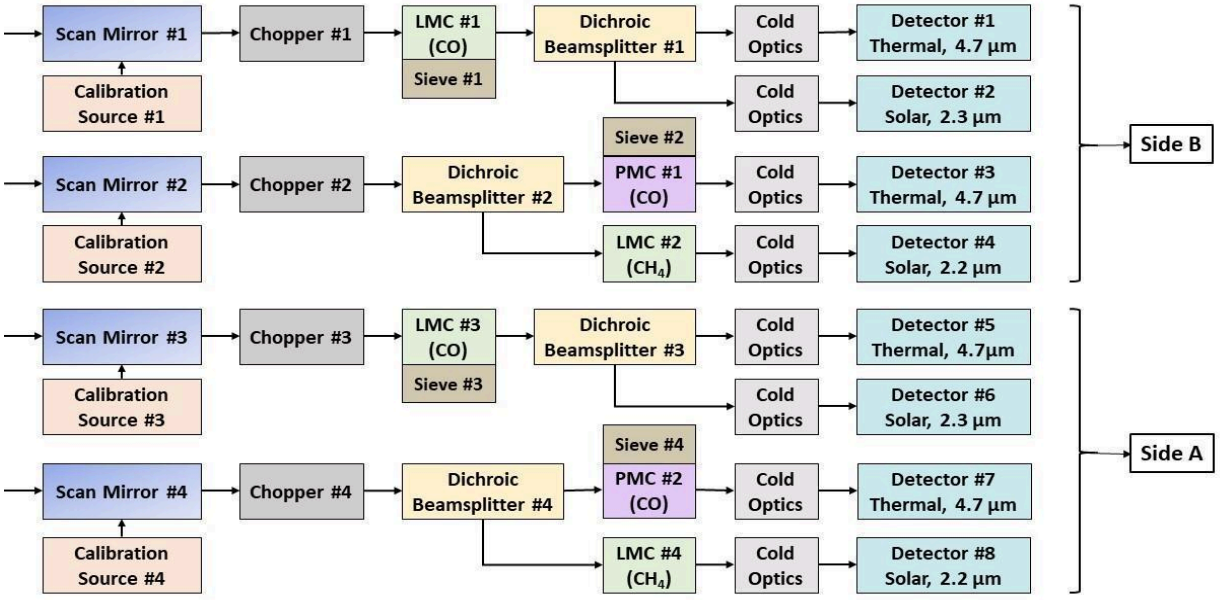

Figure 2.2.4 MOPITT optical channel diagram. Note that Side B is no longer functional due to the May 7 2001 cooler malfunction. Side A (Channels 5-8) continue to operate successfully. On August 2024, PMC #2 failed and remained off for the duration of the mission.

Table 2.2.1 MOPITT Channel characteristics.

Gas Species	CO	CO	CO	CH_4	CO	CO	CO	CH_4
Gas Pressure (kPa) (at launch)	20	20	7.5	80	80	80	3.8	80
Gas Pressure (kPa) 2020	N/A	N/A	N/A	N/A	56	56	3.2	56
Mid-band Wavenumber (cm^{-1})	2166	4285	2166	4430	2166	4285	2166	4430
Band width (cm^{-1})	52	40	52	139	52	40	52	139
Mid-band Wavelength (µm)	4.617	2.334	4.617	2.258	4.617	2.334	4.617	2.258
Band width (µm)	0.111	0.022	0.111	0.071	0.111	0.022	0.111	0.071
Modulator Type & Number	LMC1	LMC1	PMC1	LMC2	LMC3	LMC3	PMC2	LMC4
Modulator Freq (Hz)	11.78	11.78	51.85	11.78	11.54	11.54	42.85	11.54
Chopper Freq (Hz)	518.5	518.5	518.5	518.5	600	600	600	600
Scan Mirror/ Chopper Number	1	1	2	2	3	3	4	4

Calibration Source	1	1	2	2	3	3	4	4
Optical Table Side	B	B	B	B	A	A	A	A

3.0 Algorithm Descriptions

The description of the Level 0 to Level 1 processing will begin with a discussion of required inputs to the geolocation and calibration algorithms and brief descriptions of MOPITT instrument operations and its optical system. This will be followed by a detailed discussion of theoretical and practical aspects of the algorithm.

3.1 Derivation of Pixel location

The locations of observation points (pixels) on the surface of the earth are computed by combining knowledge of the MOPITT scan mirror position with spacecraft orbit and attitude information. Scan mirror positions are measured relative to a "reference" bore-sight axis by means of digital shaft encoders. Calibration of the encoders and mapping of the four pixel positions relative to the bore-sight are part of the pre-flight instrument characterization. The position of the MOPITT "reference" bore-sight axis relative to the spacecraft coordinate system was measured during integration of the instrument onto the spacecraft.

During flight, the mirror angles, as measured by the shaft encoders, are part of the Level-0 data stream at the time of each observation. The view directions of the pixels in the spacecraft coordinate frame are computed by combining the encoder outputs with the fixed "offset" of the reference bore-sight to the spacecraft axes. Geolocation is then accomplished by use of standard subroutines available in the Product Generation System (PGS) tool kit (NASA EOS Document 194-809-SD4-001). These routines include; coordinate transformation utilities which provide conversion from the spacecraft reference frame to the Earth Centered Inertial (ECI) frame and transformation from ECI to geodetic coordinates.

Other auxiliary information necessary for interpretation of the measurement at the pixel location is likewise obtained from standard utilities in the PGS tool kit. These include: (1) solar zenith angle, (2) height of terrain, and (3) surface codes indicating land, sea or coastline.

3.2 Theoretical description of radiometric calibration

The first step in the data processing of the MOPITT instrument is the conversion of the science data stream values, which reflect the output of the analog-to-digital converters, into calibrated radiances. The fundamental assumptions of the calibration procedure are:

- All emissions within the instrument obey Planck's Radiation Law.
- The optical system obeys Schwarzschild's equation.
- The optics, detector and electronic systems are linear.
- Temperatures drift slowly and are monitored.

The two required radiances are:

- The average signal over the two states of the correlation cell.
- The difference signal between the two states of the correlation cell.

The optical system has twelve states (see below). The driver behind such a complex set of states is the need to counteract two significant causes of systematic error in the instrument:

- Temperature drifts in all optical components. This is particularly a problem for the 4.7 μm channels. These are short-term variations and tend to be cyclic or random in nature.
- Long-term drifts in the system transfer function (gain) and in the electronic offsets. These are due to changes in the optical system, the detector system and the electronic system. These tend to be systematic over long (month-years) periods of time.

An overall "road map" of the Level 0 → 1 processing is shown in Figure 3.2.1 which should be consulted along with the following description.

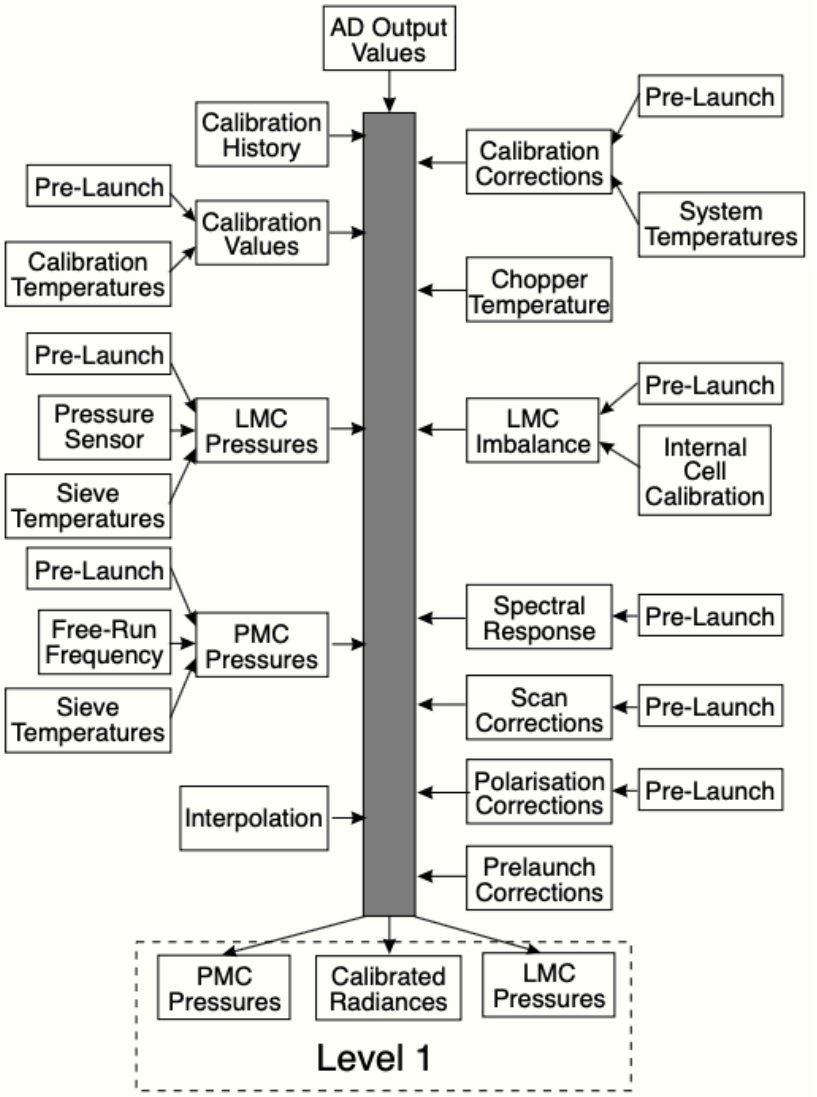

Figure 3.2.1. Level 0 to Level 1 flow processing. AD output values are the data from analog to digital converters that are delivered as Level 0 to the MOPITT SIPS.

3.2.1 Physics of the Problem

INPUTS TO THE LEVEL 0 → 1 ALGORITHM

- Count outputs from the signal channel analog-to-digital converters (one per channel).
- PRT and calibration voltage outputs for calibration sources at previous and future calibration times.
- PRT and calibration voltage outputs for chopper and molecular sieve units.
- Thermistor analog-to-digital and calibration voltage outputs of correlation cells.
- Encoder outputs for the scan mirrors.
- Sampling totals for the analog-to-digital converter accumulators.
- Spacecraft position.
- Spacecraft attitude.
- Time of measurement.

INSTRUMENT OPERATIONS

The operation of the instrument can be described as follows. A series of earth views is taken with a set period of view. The scanning system combined with the spacecraft forward motion moves this view across the planet such that the center of a given view in all channels is collocated. These views are denoted as EARTH views. After every five scans data collection is interrupted and a SPACE view is collected. Every five minutes, a view of the INTERNAL black body is taken as calibration points. During most calibration sequences the calibration blackbodies are maintained close to or at the instrument base plate temperature (short calibration) but on a roughly annual basis, the blackbodies are elevated to above 400 K for a short-wave calibration (hot calibration). This scanning sequence is illustrated in Figure 3.2.2.

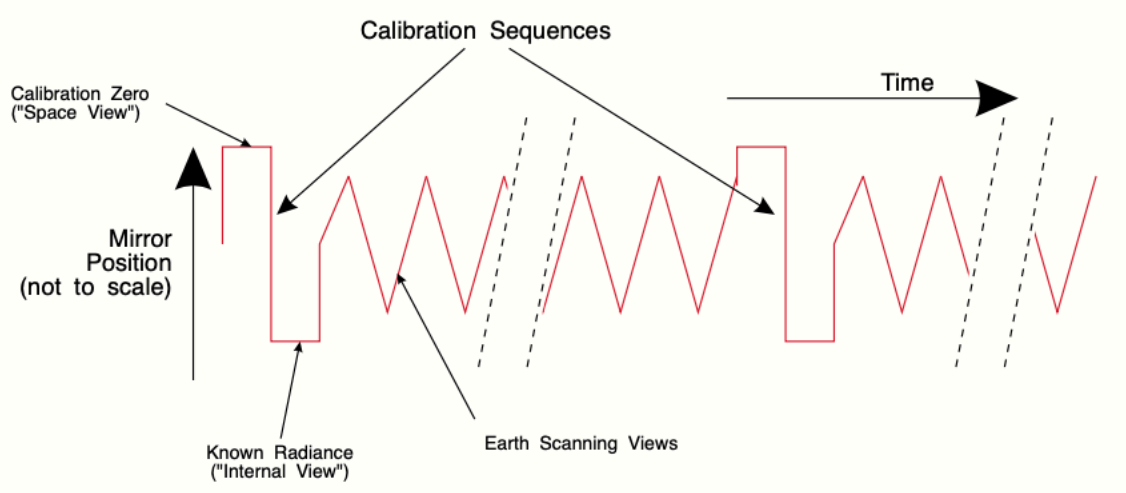

Figure 3.2.2 Typical MOPITT scanning sequence.

Each dwell time in the scan is called a "stare" and all data processing is done in units of a stare. A stare view time is 0.4 s in length with 0.054 s between stares. The inter-stare time exists to permit the data-processing system time to read out the signals and the mirror time to step and settle. However, all data is considered on a stare basis even if the mirror does not move. Thus a view of a calibration target may be described as "32 stares" implying that there will be 32 data units 0.4 s in length to be averaged for that radiance input.

OPTICAL SYSTEM DESCRIPTION

A simplified diagram of a single channel optical system is shown in Figure 3.2.3. Monochromatic radiation striking the input mirror of the optical system within the field of view (FOV) of the instrument is transferred to the detector through an optical system with a finite transmission. At the same time the optical system emits radiation within the FOV which is also relayed to the detector with an effectiveness which varies with the position of the emitting component in the optical train.

It should be recognized that the input radiance has a strong spectrally varying component and the presence of the correlation cells implies that this is also true for the optical system.

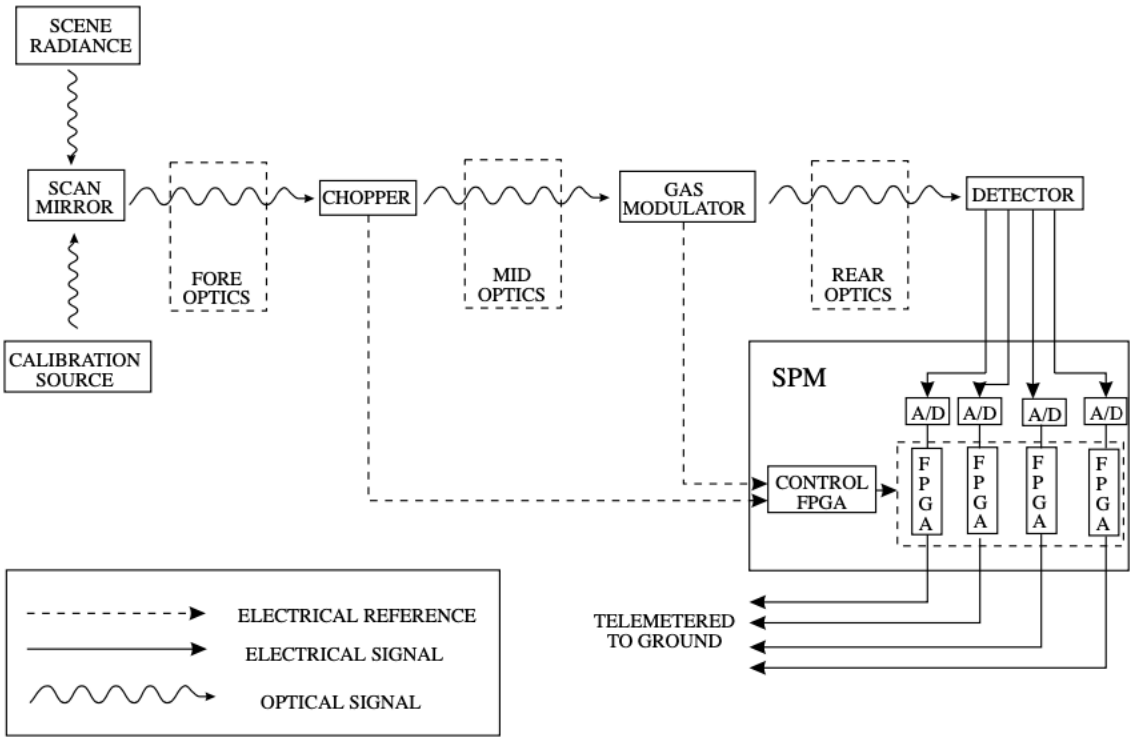

Figure 3.2.3 Single channel optical functional diagram.

SYSTEM CHOPPING AND CORRELATION CELL MODULATION

Two mechanisms cause the optical system to change its configuration with time: the correlation cell and the "chopper". The correlation cell is a cell of gas whose physical state (either pressure, for a pressure modulator cell (PMC) or length (LMC)) is modulated at a known rate in a known manner. The purpose of this cell is to produce a signal which is indicative of radiance around the absorption lines of the cell gas alone. In this analysis the correlation cell is considered as a device with two states, generically referred to as the UP and DOWN states. This description is adequate for the LMC, but in practice a more detailed model of the PMC will be required. Modulation rates are approximately 20 Hz for LMCs and 40 Hz for PMCs.

The chopper is used to partially eliminate the instrument emission signals from the problem. It consists of a blade which blocks the input beam and substitutes a known radiance (the back of the chopper blade) for the input radiance. The measurement of a known radiance at frequent intervals enables the changes in the instrument emission signals to be monitored.

The chopper in MOPITT is a rotating chopper, and this fact is used advantageously to make the chopping asymmetric (the OPEN time is longer than the CLOSED time). This is done to minimize the noise contributions from the two states. For some channels the noise in the OPEN state is higher due to the increased photon flux and for nearly all channels the smoothing of the CLOSED states (see below) effectively decreases the noise.

The total (OPEN + CLOSED) chopping interval is about 1.6 ms per cycle. This fast interval is also linked to the data acquisition system and to the correlation cell rates, thus all rates are synchronized for optimum data collection.

In August of 2001, one of the choppers froze; however, luckily it was stuck in the open position. We reformulated the radiance calculations without subtracting out the chopper-closed stares for the affected channels.

DATA ACQUISITION

The data acquisition system in MOPITT is designed to be as stable as possible which implies a high digital content. The signals are amplified and minimally filtered before being digitized and averaged over the chopper OPEN and chopper CLOSED situations. The averages are taken during the period of OPEN and CLOSED only, with the specific gating being applied to eliminate transitional data. This restricts the data taken, but ensures that they are stable and valid at all times.

The analog-to-digital converter samples at an extremely high rate (about 320 kHz) but this rate is reduced to one sample per sector internally by the Signal Processing Module (SPM) in MOPITT, achieved by summing a large number of samples. This total, along with the knowledge of how many samples are being summed, becomes the signal for the chopper state. The signals transmitted to the ground system are:

- For a PMC the sum of the chopper OPEN and chopper CLOSED states for each of the PMC UP and DOWN states for one stare (4 signals/stare).
- For an LMC the sums of the chopper OPEN and chopper CLOSED states for each of the LMC sectors in the stare (16 signals/stare). The interpolation of this to 4 signals/stare is discussed below.

The two sums just listed are converted to average values as part of the processing after the signals are received on the ground. Because the detector output is sampled only when the chopper is fully open, or fully closed, there is no chopping factor that enters into the L0 to L1 processing.

INPUT RADIANCES

The discussion in the following sections is deliberately presented in terms of radiances, since the radiances are the relevant quantities. A highly simplified optical diagram is shown in Figure 2.2.4. The corresponding equation for the signal *S*, integrated over the filter frequency band, at any time with the chopper OPEN is:

$$S = \frac{G}{T_o}\int \{([L_{input}\tau_1 + L_1]\tau_2 + L_2)\tau_g\tau_3 + L_3\}\tau_4\tau_f dv + F \qquad \text{Eqn. 1}$$

where To is the time the chopper is open, L_{input} represents the input radiance, L_1, L_2, L_3 represent the system emissions from before and after the chopper and correlation cell, τ_1, τ_2, τ_3, τ_4 the broadband optical transmissions, τ_g the gas transmission of the correlation cell, τ_f the normalized filter transmission, G the system gain and F the system offset. With the chopper CLOSED the equation becomes:

$$S = \frac{G}{T_c}\int\{([L_{chopper}\tau_1 + L_1]\tau_2 + L_2)\tau_g\tau_3 + L_3\}\tau_4\tau_f dv + F$$

Eqn. 2

where Tc is the time the chopper is closed.

Therefore, the signal observed at any instant in time can be considered to be a combination of emission from the instrument and the input signal to the optics with appropriate weighting of the two terms. This weighting varies with the state of the optics, scanning and time. By measuring the variation of the signal with optical state and understanding the mechanisms which cause the variation, the input signal alone can be deduced.

As an example of the process of elimination of the instrument terms, consider the case where the emission signals L_2 and L_3 are stable on the time scale of the chopper. The above equations can be differenced to get the "chopper difference signal" (CDS) ΔS:

$$\Delta S = G\int\{([L_{input}\tau_1 + L_1 - L_{chopper}]\tau_2\,\tau_g\tau_3\,\tau_4\tau_f dv$$

Eqn. 3

The terms L_1 and $L_{chopper}$ will be eliminated in the next step of the calibration process using the calibration sources.

Overall, each channel of input has twelve states and twelve radiances from which two representations of the input signal are derived. The twelve states are:

State	Chopper Condition	Correlation Cell Condition	Scan Condition
1	OPEN	UP	EARTH
2	CLOSED	UP	EARTH
3	OPEN	DOWN	EARTH
4	CLOSED	DOWN	EARTH
5	OPEN	UP	SPACE
6	CLOSED	UP	SPACE
7	OPEN	DOWN	SPACE
8	CLOSED	DOWN	SPACE
9	OPEN	UP	INTERNAL CAL
10	CLOSED	UP	INTERNAL CAL
11	OPEN	DOWN	INTERNAL CAL
12	CLOSED	DOWN	INTERNAL CAL

The definitions for the various mechanism states are:

Chopper [OPEN]. Chopper is fully clear of the optical system.

Chopper [CLOSED]. Chopper fully blocks incoming radiation.

Correlation Cell [UP (DOWN)]. For a length modulator cell (LMC), this refers to the short (long) path condition. For a pressure modulator cell it refers to the condition with the piston above (below) the average time point. The average time point in turn is the point at which the piston spends 50% of the time above and 50% of the time below.
Scan Condition [EARTH]. Scan system is disposed so that the input radiance comes from some part of the planet; these data are the ones required.
Scan Condition [SPACE]. The instrument scanning system uses the side ports to direct the view to space. The input radiance is effectively zero under these conditions.
Scan Condition [INTERNAL CAL]. The instrument scanning system directs the view into the appropriate on-board calibration blackbody.

CHOPPER DIFFERENCE SIGNALS (CDS)
The individual signals are first differenced to form six CDSs:

State	Signal	Correlation Cell Condition	Scan Condition
1,2	$S_{1,2}$	UP	EARTH
3,4	$S_{3,4}$	DOWN	EARTH
5,6	$S_{5,6}$	UP	SPACE
7,8	$S_{7,8}$	DOWN	SPACE
9,10	$S_{9,10}$	UP	INTERNAL CAL
11,12	$S_{11,12}$	DOWN	INTERNAL CAL

These differences are taken to eliminate instrument emission terms due to temperature drifts in the optical components. They only eliminate emission terms on the detector side of the chopper and only then if the rate of change of the emission signal is insignificant on the signal scale during a single chopper cycle. Since the chopper cycle is about 1.6 ms and the emission change with temperature is on a scale where 1 mK is small, temperature drifts of a fairly large magnitude can be suppressed.

The chopper closed signals have a number of properties which make a more sophisticated analysis appropriate:

- When the chopper is closed the instrument has no radiance input from outside and therefore can be expected to show the same signals for the same outputs from the internal temperature monitors within some fairly close limits.
- The chopper closed system input radiance is approximately the chopper blade temperature which is closely monitored. Thus although the $L_{chopper}$ term varies, the variations may be tracked through knowledge of the chopper temperature and the Planck function.

Thus, the chopper closed signals can be smoothed through a period greater than one stare, potentially reducing the noise level on the signal and changes in the chopper closed signal can be explained by changes in the chopper temperature. These properties permit the thermal offsets of the instrument (the fast changing terms) to be better monitored since they are seen on the chopper time scale.

The variations in the stray radiance from the input optics L_1 may be tracked by monitoring the temperature of the scan mirror and the surroundings. Changes in the emission over the short-term can be compensated for, but longer term changes require a full calibration.

3.2.2 Mathematical Description

DERIVATION OF AVERAGE AND DIFFERENCE SIGNALS

The average signal may be derived by taking the CDSs and then averaging over the states of the correlation cell during the stare period. e.g. $(S_{1,2}+S_{3,4})/2$.

The difference signal can be derived by taking the average of the difference of the CDSs for the two states of the correlation cell. e.g. $S_{1,2}-S_{3,4.}$

Attention must also be paid to the fact that the correlation cells also differ slightly in operation and in input signal characteristics.

The Pressure Modulator cells are treated on a "stare" basis as in the above description. All state signals are averaged over the stare time before being processed. The Length Modulator cells are treated differently for two reasons:

- The cell consists of four sectors, two "up" and two "down" which are used in sequence. Four complete rotations make up one stare time. The sectors are telemetered separately to permit individual interpretation.
- The signal may vary significantly over a "stare" time and care is required in the averaging. This is primarily because the sectors correspond to slightly different times of observation. Using the separately telemetered sectors, a cubic polynomial is fitted through the four points of each sector permitting a better estimate of the time-weighted mean of the stare than a simple average would provide. The two center-time "up" states are then averaged as are the two center-time "down" states to produce similar signals to the PMC channels.

A correction is applied at this point for the LMC channels to account for the fact that the cell rotors have slightly different transmissions in the two states and this causes an offset signal to appear in addition to the gas effect. This offset was calibrated before launch and is also monitored during a long calibration sequence by the use of an internal gas cell which is placed in the beam. By altering the relationship between the average and difference signal, the offset is highlighted and can be monitored for changes. The six signals are now:

Signal	Scan Condition
Average	EARTH
	SPACE
	INTERNAL CAL
Difference	EARTH
	SPACE
	INTERNAL CAL

CALIBRATION OF THE DIFFERENCE AND AVERAGE CHANNELS

Although the calibration of the MOPITT instrument is a total operation, it is convenient to split the discussion into two parts: the derivation of the offset terms, L_1 and $L_{chopper}$ and the determination of the transmission terms.

We begin with the derivation of the offset terms. These are determined by looking through the SPACE port at which time L_{input} is zero and equation (3) becomes:

$$\Delta S_{space} = G \int \{([L_1 - L_{chopper}]\tau_2 \tau_g \tau_3 \tau_4 \tau_f dv \qquad \text{Eqn. 4}$$

and the expression for the CDS becomes:

$$\Delta S = G \int \{([L_{input}\tau_1]\tau_2 \tau_g \tau_3 \tau_4 \tau_f dv + \Delta S_{space} \qquad \text{Eqn. 5}$$

Since the radiance terms, which are temperature dependent, can change rapidly, under certain scenarios this part of the calibration may be performed more frequently than the part of the calibration which is used to determine the gain and transmission terms.

The term ΔS_{space} is evidently a function of the chopper and front optics radiances. Since these are carefully monitored it is possible to interpolate space signals between the actual measurement times using these temperatures to determine the variations.

The cold calibrations (or Space Views) occur after every five scans or approximately every two minutes. The duration is five stares or ~2.5 seconds. Warm calibration events (or Internal Views) where the mirror is pointed at the internal black body occur approximately every 11 minutes. The mirror fixed on the black body for 20 stares. The stares are averaged to give a single warm and cold calibration value. The standard deviation of these stares is used to calculate the instrument noise because we assume the target is stable during the calibration event.

The next computation is essentially the determination of the channel GAIN using the INTERNAL signal as a known radiance, followed by the application of these values to the EARTH signals. This leads to the general equation:

$$L_{earth} = L_{internal}\left(\frac{\Delta S_{earth} - \Delta S_{space}}{\Delta S_{internal} - \Delta S_{space}}\right) \qquad \text{Eqn. 6}$$

This formula is applied to both the average and difference channels to produce the required radiances. The internal radiance $L_{internal}$ is derived from knowledge of the temperature and emissivity of the calibration source. This uses Platinum Resistance Thermometer (PRT) sensors which are discussed below. A more sophisticated analysis can obviously be applied based on the fact that the long-term drifts are exactly that, “long term”, and the emission changes in the instrument are correlated with temperature changes. Thus we assume that all gain and offset factors change slowly compared with the calibration period and that the emission signals correlate with measured temperatures. Under these assumptions it is possible to build two additional inputs for the calibration system: an instrument characteristic emission model and a gain/offset history. Thus in determining the current radiometric calibration, the overall

radiometric calibration uses: (1) current calibration values, (2) historic calibration values, and (3) instrument temperatures.

For the NIR channels, the procedure is essentially the same except the instrument is taken out of Science Mode. The black body temperature is raised until it emits significantly in the 2.3 micron band. The mirror acquires an internal radiance value, which is used for the NIR calibration. This process is performed on a quasi-annual basis. During this period, while the instrument is not taking valid scientific measurements, other maintenance operations are performed. These are described below.

DERIVATION OF TEMPERATURES

Derivation of temperature from Platinum Resistance Thermometer (PRT) sensors is as follows:

1. Deduce the PRT resistances. The resistances are monitored by means of a potential divider circuit with a known resistor *R*, for which the input, output and zero voltages are measured in terms of analog-to-digital converter counts (N_i, N_o, N_z). The resistance R_{PRT} is therefore given by:

$$R_{PRT} = R\left(\frac{N_o - N_z}{N_i - N_o}\right) \qquad \text{Eqn. 7}$$

2. Deduce the temperature from the PRT resistance. This is a known characteristic which although approximately linear can be better represented by a low order polynomial

$$T = \sum_{i=0}^{n} r_i \left(R_{PRT}\right)^i \qquad \text{Eqn. 8}$$

The coefficients for a PRT are already well known once the type of PRT has been defined. They were also verified before launch. Derivation of temperature from thermistor sensors follows the same general path except that the formula for the resistance versus temperature characteristic is more non-linear.

DERIVATION OF CORRELATION CELL PRESSURES

Additional input required for the Level 2 data processing include the correlation cell pressures. These are required for two reasons:

- The pressure in the correlation cell affects the manner of interpretation of the Level 1 radiance(e.g., the difference signals are a strong function of cell pressure and go to zero if the cell pressure is zero).
- The cell pressure affects the shape of the weighting functions used in the Level 1 → 2 algorithm.

  The Pressure Modulator Cell has a constant cell length, but continuously changing temperature and pressure. The strategy for determining the form of the time cycles of temperature and pressure involves both pre-flight and in-flight measurements. The pressure and temperature cycles of the PMCs aboard MOPITT were determined

pre-launch using spectrometric techniques developed at the University of Toronto (Berman et al., 1993). These cycles were measured as a function of average cell pressure. In-flight, it is then necessary to determine average cell pressure in order to derive the temperature and pressure cycle. Average cell pressure can be derived in either of two ways:

1) By means of the free-run, or resonant, frequency. The frequency versus pressure relationship is constant with time for a given PMC (based on experience with several instruments such as SAMS, ISAMS, PMIRR, etc.) This relationship is characterized before launch. The resonant frequency is measured periodically in-flight (although for normal operation the PMC is driven slightly off resonance). A polynomial fit to the pre-launch data is then used to deduce the pressure, p, from the measured in-flight resonant frequency, F:

$$p = \sum_{i=0}^{n} f_i F^i \qquad \text{Eqn. 9}$$

2) By means of the sieve temperature. This is not as precise as method 1, and is subject to a number of errors (e.g., gas contamination will not show up). However, this method can be used on a continuous basis. The sieve pressure versus temperature relationship was characterized before launch. The sieve temperatures are monitored by means of PRT's in-flight. A polynomial fit to the pre-launch data is again used to deduce the pressure, p, from the measured in-flight sieve temperature, T.

$$p = \sum_{i=0}^{n} t_i T^i \qquad \text{Eqn. 10}$$

A length modulator cell is isothermal and only has two length states: "long" and "short". These lengths are measured before launch and cannot change without destruction of the LMC. The pressure can be monitored by an accurate pressure transducer on the cell and also (less precisely) by the temperature of the sieve system (CO cells only). The sieve temperature technique is as described above. The pressure sensor mounted on the LMC is strain gauge based. It has its own electronic processing, and produces a voltage which is (almost) proportional to the pressure. Thus, the calibration proceeds in two stages:

1. Deduce the voltage V from measurements of the voltage, a reference voltage V_r, and the zero voltage V_z measured in terms of converter counts (N, N_r, N_z):

$$V = \left(V_r - V_z\right)\left(\frac{N - N_z}{N_r - N_z}\right) + 2\,V_z \qquad \text{Eqn. 11}$$

2. Using pre-flight calibration data, relate the measured voltage to the pressure using a polynomial fit:

$$p = \sum_{i=0}^{n} v_i V^i \qquad \text{Eqn. 12}$$

The balance error of the cell also needs to be measured. This can be done by a pre-launch measurement supplemented by in-flight calibrations using the MOPITT blackbodies. Corrections for the spectral distribution of the blackbodies and known pressure dependent effects (reflection losses at the interfaces) in the system are also required.

3.2.3 Variance and Uncertainty Estimation

The accuracy of the calibrated radiances is related to the measurement of the input radiance in terms of the calibration sources followed by their traceability to international standards. The calibration will initially be established in the Instrument Calibration Facility (ICF). The current specifications are:

Long wave (4.7 μm) channels: ±0.5 K.

Short-wave (2.3, 2.4μm) channels: ±1 K.

Measured values for the variance and uncertainty will be available after calibration tests are performed on the engineering model of MOPITT. These will be far more valuable than any calculated values for the purpose of assessing instrument performance.

A note of caution is that the radiances are computed in the same manner as for a broad-band radiometer. However the nature of the spectral response of a correlation instrument is very different and caution should be exercised when comparing these radiances to radiances from a true broad-band radiometer. Further information is contained in the MOPITT Calibration Plan.

The resolution or repeatability of the MOPITT calibration is governed by a number of factors, some of which have a short characteristic time scale and some of which have a longer characteristic time. The objective of MOPITT is to measure gas concentrations in the atmosphere, not necessarily radiance. A detailed analysis of this objective shows that the repeatability of MOPITT measurements are, over the long term, more important than the accuracy of the initial calibration.

The short-term resolution of the MOPITT calibration is governed by a number of factors, the first of which is the noise level associated with the calibration itself. This can be adjusted by adjusting the length of time each target is viewed. Longer times permit better averaging of the radiance and temperature data.

Secondary factors which contribute to the calibration resolution are the applicability of the current calibration values to the radiance transformation. Temperature drifts are the primary cause of inaccuracy here and govern the time between calibration sequences. The primary elements in this operation are the chopper emissivity and temperature, which are both carefully controlled and, in the case of the temperature, carefully monitored. The governing time is that time in the middle of which the uncertainty in the corrections grows to a level which prejudices the consistency of the calibration.

In practical terms the variance of the radiances can be found by using the fact that there are many calibration sequences that are measurements of known radiances and that the major features of the calibration (optical transmission, etc.) change slowly with time. Thus daily, weekly, monthly and annual estimates of the changes in calibration parameters from the calibration history give valuable information on the variance of the calibration parameters and their drift with time.

4.0 On-orbit lessons learned and corrections

4.1 Calibration of Near Infrared Channels

Revisions to the calibration method of the NIR channels is discussed in detail in section 3.6 of the V9 User's Guide. See
https://asdc.larc.nasa.gov/documents/mopitt/guide/v9_users_guide_20220203.pdf

4.2 What Happened to the Methane Observation?

Variations in surface reflectance as the satellite traversed the Earth added so much noise during each stare that methane retrievals were deemed to be scientifically unreliable. Uniform surface conditions such as oceans mitigated that problem although oceans were too dark in the NIR band to provide a strong enough signal. The methane retrievals were abandoned. The L1 calibrated radiance data for the methane channels is preserved in the data for future exploration.

Appendix A. Timeline of events

Date	MOPITT Activity	Instrument Anomaly Description
1999/12/18	Launch	
1999/12/18 - 2000/02/28	Survival/Safe/Standby modes (initial outgas/activation)	
2000/02/28	Doors opened	
2000/03/02	Coolers on, Science mode	
2000/03/07 - 2000/03/22	B&P tests, Hot calibration (03/22, 03/23)	
2000/03/23 - 2000/07/04	Science mode	

2000/07/04 - 2000/07/14	Hot calibration, decontamination and Hot calibration (07/12, 07/13)	
2000/07/14 - 2000/11/12	Science mode	
2000/11/12 - 2000/11/17	Hot calibration (11/14), baseline LMC and burstmode data	
2000/11/17 - 2001/2/6	Science mode	
2001/02/04 - 2001/02/15	Hot calibration, decontamination and Hot calibration (02/15, 02/16)	
2001/02/16 - 2001/05/06	Science mode	
2001/05/07	Side B Cooler Failure (channels 1-4 no longer usable)	MOPITT used two coolers, each of which were composed of a linear compressor motor and a linear displacer motor, connected with a gas tube. A cold finger mounted on the displacer was used to achieve detector cooling, and the two coolers were operated in anti-phase to minimize compressor-driven vibrations. In May 2001, the side B displacer hit the end stop, causing the cooler subsystem to shut down. Diagnosis revealed that the side B displacer was unresponsive to commands but was being driven by pressure waves from the side B compressor. This inhibited cooling to the side B detectors (channels 1-4), rendering their measurements non-viable. Due to the anti-phase operations of the twinned coolers, cooler A could not be operated independently which would cause vibrations in the system. Thus, operation of the side B compressor was adjusted to compensate for vibrations from compressor A, while maintaining a maximum amplitude low enough to avoid having the side B displacer hitting the end stop. Testing indicated that the side B compressor should be operated at 82.5% of the nominal stroke. The side A compressor was also reduced in amplitude slightly, while the Side A displacer was increased in amplitude, the combined effect being an increase in the effective cooling from side A with a reduction in the compressor-driven vibrations.

2001/08/04	Chopper 3 Anomaly (stay open)	Each MOPITT optical channel began with a chopper, designed to allow for thermal drift calibration in the instrument; however, operations showed that the spaceview is sufficient to account for thermal drift in calibrations to the first order. In 2001, chopper #3 failed, stopping completely and becoming unresponsive to further commands. Fortunately, the chopper failed in the open position. As the use of the chopper was deemed non-essential to the collection of science-quality data, this had little effect on the ongoing mission.
2001/05/07 - 2001/08/24	Standby mode and Instrument tests (no retrievals)	
2001/08/25 - 2002/03/02	Science mode: Phase 2 (with channels 5-8)	
2002/03/03 - 2002/03/04	Hot calibration	
2002/03/19 - 2002/03/25	Terra Anomaly	During March 2002, a Terra anomaly caused Terra and the instruments aboard, including MOPITT, to enter SAFE mode. The satellite was recovered and MOPITT was set back into SCIENCE mode with commanding in early March.
2002/03/28 - 2002/03/30	Hot calibration	
2002/04/06	Mirror #1 Anomaly	In April 2002, Mirror 1 completely failed, becoming unresponsive to commands. As this was on the non-operating side B of MOPITT this did not affect the collection of science data.
2002/11/30 - 2002/12/12	Hot calibration, decontamination and Hot calibration (12/12)	
2002/12/13 - 2002/12/18	Standby mode (cooler off)	In December 2002, the MOPITT side B displacer hit the end stop, causing a cooler shutdown. The cooler subsystem was brought back online with the same settings as after the May 2001 cooler subsystem failure. While the side B detectors remained non-operational due to their temperatures, scientific operation of the side A detectors continued after this anomaly with little impact.

2002/12/19 - 2003/12/12	Science mode	
2003/12/13 - 2004/01/02	Anomaly, decontamination and Hot calibration (2004/01/02)	During December 2003, a Terra anomaly for an out-of-limits yaw rate caused Terra and the instruments aboard including MOPITT to enter SAFE mode. The satellite was recovered and MOPITT was set back into SCIENCE mode with commanding in early January.
2004/01/03 - 2004/06/08	Science mode	
2004/06/09 - 2004/06/10	Hot calibration	
2004/06/11 - 2005/01/18	Science mode	
2005/01/19 - 2005/01/20	Hot calibration	
2005/01/21 - 2005/04/24	Science mode	
2005/04/25 - 2005/05/05	Hot calibration, decontamination and Hot calibration (05/04, 05/05)	
2005/05/06 - 2006/10/01	Science mode	
2006/10/02 - 2006/10/14	Hot calibration, decontamination and Hot calibration (10/14)	
2006/10/15 - 2008/01/28	Science mode	
2008/01/29 - 2008/02/09	Hot calibration (01/30) and decontamination	
2008/02/10 - 2009/01/30	Science mode	
2009/01/31 - 2009/02/11	Hot calibration, decontamination and Hot calibration (02/10)	
2009/02/12 - 2009/07/27	Science mode	
2009/07/28 - 2009/09/29	the third Cooler Anomaly (no science data)	In July 2009, the MOPITT side B displacer hit the end stop, causing a cooler shutdown. The cooler subsystem was brought back online into a similar state as it had been since the 2001 cryocooler failure but with a slight reduction in the side B compressor amplitude, to 77.5 %. While the side B

		detectors remained non-operational due to their temperatures, scientific operation of the side A detectors continued after this anomaly with little impact.
2009/09/30 - 2009/10/03	Science Mode	
2009/10/03	LMC3 Sieve Heater Failure	The sieves are connected to the LMC subsystems and act to buffer against changes in pressure in the cells by changing the sieve body temperature. In October 2009, the heater for Sieve 3 turned off spontaneously, lowering the pressure in LMC 3 by about 3.2 kPa. This drop was readily accounted for in the data processing, and no impact on science data was found for this anomaly once compensated for. In March 2011, the heater for Sieve 3 turned on again and resumed nominal operations, increasing the LMC pressure, but again having no tangible effect on the science data once the change had been compensated for in the retrieval algorithm.
2009/10/04 - 2010/01/19	Science Mode	
2010/01/20 - 2010/01/21	Hot calibration	
2010/01/22 - 2011/03/13	Science Mode	
2010/12/02 - 2011/03/21	LMC1 Sieve Heater Failure	In December 2010, the heater for Sieve 1 turned off spontaneously, lowering the pressure in LMC1. As LMC1 is on the non-operational side of MOPITT, this did not affect routine scientific operations. After MOPITT was reset during the next decontamination, the heater was reactivated.
2011/03/14 - 2011/03/25	Hot calibration (03/14, 03/15), decontamination, Sieve Heater on again and Hot calibration (03/25)	In October 2009, the heater for Sieve 3 turned off spontaneously, thereby lowering the pressure in LMC 3 by about 3.2 kPa. In March 2011, the heater for Sieve 3 turned on again and resumed nominal operations, increasing the LMC pressure, but again having no tangible effect on the science data once the change had been compensated for in the retrieval algorithm.

2011/03/26 - 2012/03/04	Science Mode	
2012/03/05 - 2012/03/16	Hot calibration, decontamination and Hot calibration (03/16)	
2012/03/17 - 2013/03/24	Science Mode	
2013/03/25 - 2013/04/05	Hot calibration, decontamination and Hot calibration (04/05)	
2013/04/06 - 2014/03/23	Science Mode	
2014/03/24 - 2014/04/08	Hot calibration, decontamination, CPHTS and Hot calibration (04/08)	
2014/04/09 - 2015/03/22	Science Mode	
2015/03/23 - 2015/04/03	Hot calibration, decontamination and Hot calibration (04/03)	
2015/04/04 - 2016/02/17	Science Mode	
2016/02/18 - 2016/03/04	Terra Anomaly, decontamination and Hot calibration (03/04)	During February 2016, a Terra anomaly caused Terra and the instruments aboard, including MOPITT, to enter SAFE mode. The satellite was recovered and MOPITT was set back into SCIENCE mode with commanding in early March.
2016/03/05 - 2017/03/05	Science Mode	
2017/03/06 - 2017/03/17	Hot calibration, decontamination and Hot calibration (03/17)	
2017/03/18 - 2018/03/11	Science Mode	
2017/12/12 - 2018/03/19	LMC1 Sieve Heater Failure	In December 2017, the heater for Sieve 1 turned off spontaneously, lowering the pressure in LMC1. As LMC1 is on the non-operational side of MOPITT, this did not affect routine scientific operations. After MOPITT was reset during the next decontamination, the heater was reactivated.
2018/03/12 - 2018/03/23	Hot calibration, decontamination and Hot calibration (03/23)	
2018/03/24 - 2018/09/26	Science Mode	

2018/09/27 - 2018/10/05	Safe Mode (cooler off)	During September 2018, a Terra anomaly caused Terra and the instruments aboard, including MOPITT, to enter SAFE mode. The satellite was recovered and MOPITT was set back into SCIENCE mode with commanding in early October.
2018/10/06 - 2018/10/07	Science Mode	
2018/10/08 - 2018/10/10	Hot calibration + Terra high gain antenna (HGA) failure/recovery	
2018/10/11 - 2019/03/10	Science Mode	
2019/03/11 - 2019/03/23	Hot calibration, decontamination and Hot calibration (03/22)	
2019/03/24 - 2019/07/25	Science Mode	
2019/07/26 - 2019/08/24	SEU Anomaly recovery, Hot calibration, decontamination and Hot calibration (no valid MOPCH)	During July 2019, the Sieve 4 heater turned off, causing the PMC2 amplitude to drop. After MOPITT was rest, PMC 2 operations returned to normal, and scientific operations could continue. During the latter part of this recovery period, the first PMC 2 vibration event was observed. These irregular (both in length and frequency) events would continue to affect MOPITT until the PMC 2 failure in August 2024. During PMC 2 vibration events, no science-quality data could be obtained.
2019/08/25 - 2020/03/22	Science Mode	
2020/03/23 - 2020/04/04	Hot calibration, decontamination and Hot calibration (04/03)	
2020/04/05 - 2021/03/24	Science Mode	
2021/03/25 - 2021/04/13	Hot calibrations, decontamination and Hot calibrations	
2021/04/14 - 2022/06/05	Science Mode	
2022/06/06 - 2022/06/18	Hot calibrations, decontamination and Hot calibrations	
2022/06/19 - 2022/10/02	Science Mode	

2022/10/03 - 2022/10/29	Hot calibrations and Terra constellation exit maneuver (CEM)	
2022/10/30 - 2023/11/26	Post-CEM Science Mode	
2023/11/27 - 2023/12/09	Hot calibrations	
2023/12/10 - 2024/08/11	Post-CEM Science Mode	
2024/08/11 - 2025/02/01	PMC2 (channel 7) failure - impact to CO retrievals in upper troposphere	Beginning 19 August 2019, vibrations were observed in the MOPITT instrument originating from PMC 2. These vibration events were irregular both in duration and frequency. In August 2024, the piston position for PMC 2 began varying wildly, as did its driving current. This was accompanied by vibrations in the system reminiscent of those observed during the PMC 2 vibration events; however these vibrations were stronger in intensity. After a few hours of this irregular behaviour, the piston position became fixed, and the motor current began to increase, accompanied by an increase in PMC 2 temperatures. PMC 2 was turned off, the vibrations ceased, and the temperatures normalized. Several rounds of testing were performed, using PMC 1 as a comparison, and PMC 2 clearly illustrated that it was no longer capable of generating distinct measurement states or operating as intended. The irregularity of the piston response and the ensuing vibrations indicated that this was likely a mechanical failure. Attempts to recover PMC 2 after the MOPITT reset in November 2024 saw the issue persist to the point of a complete mechanical failure in PMC 2. This failure rendered channel 7 inoperable, but did not affect channel 5 and 6, thus permitting scientific operations to continue, albeit with a change to the measurement products.
2024/08/11 - 2024/11/11	Post-CEM Science Mode without PMC 2	
2024/11/11 - 2024/11/23	Hot calibrations	
2024/11/24 -	Post-CEM Science Mode without PMC 2	

2024/12/27		
2024/12/27	MOPITT Side B shutdown	In the latter part of the Terra mission, several solar array shunts, which connect the solar panel array to the batteries, failed and several displayed intermittent issues. Alongside this, as the orbit of Terra drifts over time there is a slow decrease in the amount of power generated from the solar panels. With the loss of the most recent solar array shunt, Terra fell into a power negative state requiring offloading some of the Terra operations. ASTER was put into hiatus in early December 2024; however, continually decreasing power margins and falling battery temperatures required further load adjustments near the end of December 2024. To help accomplish this, several of the Side B elements of MOPITT were turned off. This included Chopper#1 and #2, Mirror#1 and #2, LMC#1 and #2, Sieve#1 and #2, and PMC#1. As no observations are made with the Side B detectors, this does not affect routine MOPITT operations.
2024/12/27-2025/02/01	Post-CEM Science Mode without PMC 2	
2025/02/01	MOPITT SAFE	With continually decreasing power margins on the spacecraft, and continually falling battery cell temperatures in January, further load shedding was deemed essential in January 2025. Due to the high power consumption of MOPITT compared to the other Terra instruments, MOPITT was flagged to be put into SAFE mode in order to save on power. While in SAFE mode, MOPITT does not make scientific measurements.
2025/04/09	MOPITT OFF	Further power demands from the Terra satellite and its instruments saw MOPITT put into SURVIVAL and then finally turned OFF in April 2025, ending the MOPITT scientific data record.

5.0 References

Berman, R., P. Duggan, M. P. Le Flohic, A. D. May, and J. R. Drummond, Spectroscopictechnique for measuring the temperature and pressure cycle of a pressure modulator radiometer,Applied Optics, 32, 6280-6283, 1993.

Drummond, J. R., et al., MOPITT Mission Description Document, University of Toronto,Department of Physics, 1993.

Drummond, J. R., Novel correlation radiometer: the length-modulated radiometer, Appl. Opt.28,2451-2452, 1989.

Drummond, J. R., Measurements of Pollution in the Troposphere (MOPITT), in The use of EOS for Studies of Atmospheric Physics, edited by J. C. Gille and G. Visconti, pp. 77-101, North Holland, Amsterdam, 1992.

Drummond, J. R., J. Zou, F. Nichitiu, J. Kar, R. Deschambaut, and J. Hackett (2010), A review of 9-year performance and operation of the MOPITT instrument, *Advances in Space Research*, *45*(6), 760–774, doi:10.1016/j.asr.2009.11.019.

Mand, G. MOPITT Test Plan, MOPITT document number MOPITT-TD-0005, University ofToronto, Department of Physics, 1995.

Mand, G. MOPITT Science Test Program, MOPITT document number MOPITT-TD-0006,University of Toronto, Department of Physics, 1995.

Mand, G. MOPITT Environmental Test Program MOPITT document number MOPITT-TD-0007, University of Toronto, Department of Physics, 1995.

Pfister, G., J. C. Gille, D. Ziskin, G. Francis, D. P. Edwards, M. N. Deeter, and E. Abbott, Effects of a Spectral Surface Reflectance on Measurements of Backscattered Solar Radiation: Application to the MOPITT Methane Retrieval, *Journal of Atmospheric and Oceanic Technology*, *22*(5), 566–574, doi:10.1175/JTECH1721.1, 2005.

Reichle Jr., H. G. , V. S. Connors, J. A. Holland, W. D. Hypes, H. A. Wallio, J. C. Casas, B. B.Gormsen, M. S. Saylor, and W. D. Hesketh,Middle and upper tropospheric carbon monoxidemixing ratios as measured by a satellite-borne remote sensor during November 1981, J. Geophys.Res., 91, 10865-10887, 1986.

Reichle, Jr., H. G., V. S. Connors, J. A. Holland, R. T. Sherrill, H. A. Wallio, J. C. Casas, E. P.Condon, B B.Gormsen, and W. Seiler, The distribution of middle tropospheric carbon monoxideduring early October 1984, J. Geophys,. Res., 95, 9845-9856, 1990.

Taylor, F. W., Pressure modulator radiometry, in Spectroscopic techniques. Vol.III, pp.137-197,Academic Press Inc., 1983.